Carbon Dispersant

DOI: 10.1002/ange.201307459

The Colloidal Stabilization of Carbon with Carbon: Carbon Nanobubbles as both Dispersant and Glue for Carbon Nanotubes**

*Danuta Kuzmicz, Simon Prescher, Frank Polzer, Sebastian Soll, Christoph Seitz, Markus Antonietti, and Jiayin Yuan**

Abstract: *The superior physical properties of carbon nanotubes (CNTs) have led to their broad application. Intrinsically, CNTs tend to agglomerate from hydrophobic interactions, which is highly undesirable for solution processing and device fabrication. Commonly, a stabilizer consisting of organic surfactants or polymers is used to disperse CNTs. Recently, we synthesized nitrogen-doped carbon hollow nanospheres (25–90 nm), termed carbon "nanobubbles". They bear superior dispersability in water and distinctive graphitic order. Herein, we describe the nanobubble-assisted dispersion of CNTs in aqueous solution upon sonication. This process relies on the π–π interaction between the two aromatic carbon nanostructures, which can process their carbon mixture in water into conductive filter membranes, ink, and discs. This stabilization can be extended to other aromatic carbons. In addition, the π–π interaction may create a new type of carbon p–n junction that can be used to improve charge separation.*

Owing to their unusual electrical, mechanical, optical, thermal, and chemical properties, carbon nanotubes (CNTs) have found tremendous applications in many fields, including nanoelectronics,[1] drug delivery,[2] composite devices of different types,[3] and optical sensors.[4] Intrinsically, CNTs tend to agglomerate into bundles during preparation because of hydrophobic interactions. This heavily agglomerated state is highly undesirable and causes difficulties in solution processing. A solution to this problem is to disperse CNTs with a stabilizer or deagglomeration agent. Two state-of-the-art approaches are well-known: the covalent and the physical. The former is based on chemical modification of the CNT surface, typically involving the covalent attachment of organic molecules onto the carbon surface to solubilize the material. A disadvantage associated with this method is the undesirable disruption of the π conjugation network in the CNTs, especially in single-walled CNTs (SWCNTs), undermining both the mechanical and electronic properties. The physical method relies on mixing the CNTs with an excess of stabilizer, usually organic surfactants, DNA, or other polymers, which noncovalently bind to the carbon surface. In such a manner, the original bulk properties of CNTs are well preserved. However, the massive amounts of organic stabilizers constitute a heterophase impurity and are a concern in all applications, for example in electrochemical or high temperature operations.

Porous carbon nanostructures in various morphologies and heteroatom doping have attracted rapidly expanding interest and have been heavily studied in the last decade because of their unique and superior properties. Their applications in energy storage, catalysis, sorption, and sensing, have been demonstrated.[5] Very recently, we reported the synthesis of nitrogen-doped carbon hollow nanospheres, termed "nanobubbles" (CNB-*y*, where *y* indicates the size). These CNBs have distinctive graphitic order, high conductivity, variable nitrogen content and controlled dimensions (25–90 nm).[6] A striking property of this unique aromatic carbon nanostructure is its superior dispersability in neutral water, which was attributed to spontaneous charge transfer and hydroxylate adsorption. In this contribution, we describe, as an expansion of this effect, the CNB-assisted dispersion of CNTs in aqueous solution upon sonication, as illustrated in Scheme 1. This process relies on the π–π interaction between the relatively electron-poor CNBs and the electron-rich CNTs, which allows the mixture to be processed in water to produce conductive filter membranes, and purely carbon-based ink and discs without the necessity of other additives.

The dispersion experiments were performed by adding a defined amount of CNT powders to an aqueous dispersion of CNBs under sonication (Sonorex RK 100 ultrasonic bath for 2 h). The CNB content in the dispersion was determined prior to the dispersion experiments (see the Supporting Information). In this study, SWCNTs and multi-walled CNTs (MWCNTs) were both employed. As for CNBs, two different sizes (25 and 90 nm; CNB-25 and CNB-90, respectively) with the same nitrogen content (4.5 wt%) were tested. During sonication, the bottom layer of CNT powder slowly vanishes, and the dilution of the upper mixed dispersion resulted in an

[*] Dr. D. Kuzmicz, M. Sc. S. Prescher, Dr. S. Soll, Prof. M. Antonietti, Dr. J. Yuan
Max Planck Institute of Colloids and Interfaces
Am Mühleberg 1, 14476 Potsdam (Germany)
E-mail: jiayin.yuan@mpikg.mpg.de
Dr. F. Polzer
Institut für Physik, Humboldt-Universität zu Berlin, AG TEM
Newtonstrasse 15, 12489 Berlin (Germany)
C. Seitz
Institute of Physical Chemistry, Justus Liebig University of Giessen, Heinrich-Buff-Ring 58, 35392 Giessen (Germany)

[**] The authors thank Mr. Michael Koebe, Mr. Henryk Pitas, Prof. Bernd M. Smarsly, and Prof. Zhixiang Wei for their help in the synthesis, instrumental setup and fruitful discussions. This project was financially supported by the Max Planck Society and the international joint laboratory program between the Max Planck Institute of Colloids and Interfaces in Potsdam (Germany) and the National Center for Nanoscience and Technology in Beijing, China. Dr. Frank Polzer would like to thank the CRC 951 of the Deutsche Forschungsgemeinschaft and the Joint Lab for Structural Research Berlin for funding.

Supporting information for this article is available on the WWW under http://dx.doi.org/10.1002/anie.201307459.

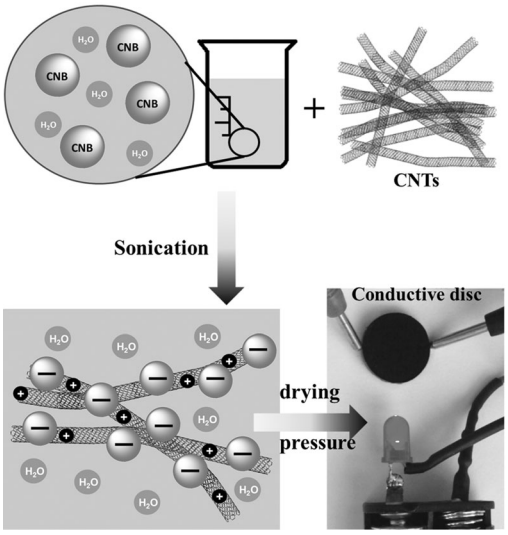

Scheme 1. Stabilization of carbon nanotubes (CNTs) by water-dispersible carbon nanobubbles (CNBs) in the aqueous phase, and the preparation of the CNT/CNB composite conductive disc.

optically transparent, grey dispersion. This dispersion remained stable for at least 20 days, although a small fraction of precipitate was observed on the bottom after 2 h. By gentle shaking, the precipitate entered into dispersion again. Sonication treatment of CNTs without the assistance of CNBs was also performed. We observed that MWCNTs precipitated in 2 min, whereas most SWCNTs precipitated in the first 2 min and the rest in the next 10 min.

The dispersion samples were subjected to transmission electron microscopy (TEM) characterization (Figure 1). Figure 1 a,b shows the morphology of CNB-25 and CNB-90, respectively. In Figure 1 c,d, CNB-25 is shown to bind specifically to the surface of MWCNTs and SWCNTs. Some free CNBs, which were separated from CNTs, were observed, whereas most investigated CNTs were indeed attached to CNBs in an irregular manner. This scenario resembles a typical surfactant-introduced stabilization phenomenon, in which only a portion of excessively added stabilizers attach to the carbon surface. The same behavior was also found when CNTs were mixed with CNB-90 under sonication treatment (Figure 1 e,f). This observation already speaks for an unusual fact that the CNBs seem to strongly adhere to the nanotube surface, thus promoting the overall hydrophilicity of the CNTs, which enables dispersion in water.

In TEM characterization, a capillary effect during drying might change the structure of the assembly. To exclude this artifact, cryogenic TEM (cryo-TEM) characterization was also performed to support the TEM analysis. Figure 2 displays photographs (24 h after sonication) of vials filled with aqueous dispersion of MWCNTs, CNB-90, and a mixture of both at low and high concentrations. As expected, pristine MWCNTs precipitate out quickly in the absence of stabilizer (0.05 mg mL^{-1} in Figure 2 a), whereas the CNB-90 dispersion (0.1 mg mL^{-1} in Figure 2 b) remains stable. In the case of the MWCNT/CNB mixtures, an interesting concentration-dependent colloidal stability was noticed. At low MWCNT concentration (0.05 mg mL^{-1}), the dark dispersion appeared homogeneous and only a small fraction was detected at the bottom (Figure 2 c). As discussed below, this precipitate was

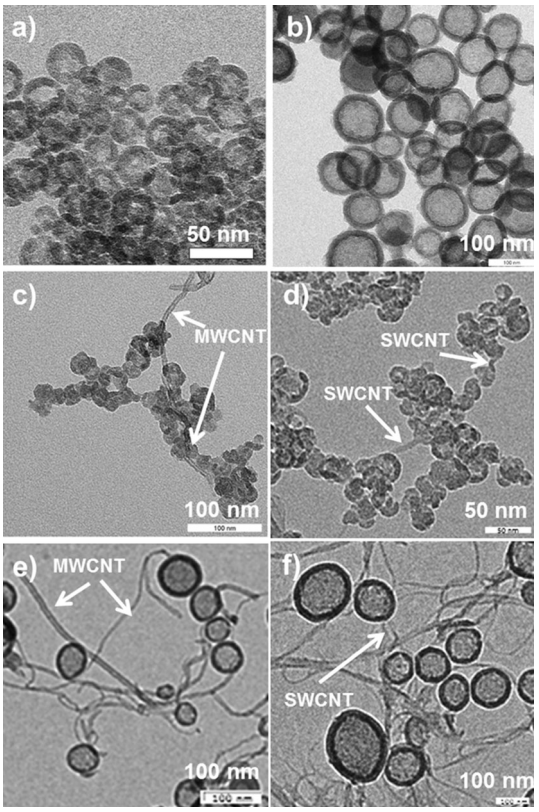

Figure 1. TEM images of the aqueous-dispersion samples of a) CNB-25, b) CNB-90, c) CNB-25 (0.06 mg mL^{-1}) with MWCNTs (0.01 mg mL^{-1}), d) CNB-25 (0.06 mg mL^{-1}) with SWCNTs (0.01 mg mL^{-1}), e) CNB-90 (0.1 mg mL^{-1}) with MWCNTs (0.03 mg mL^{-1}), f) CNB-90 (0.1 mg mL^{-1}) with SWCNTs (0.03 mg mL^{-1}).

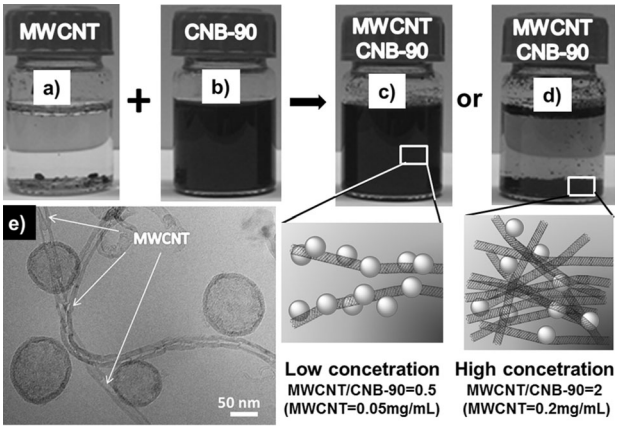

Figure 2. Photographs of vials containing aqueous dispersions of MWCNTs and CNBs, taken 24 h after sonication: a) pristine MWCNTs (0.05 mg mL^{-1}), b) CNB-90 (0.1 mg mL^{-1}), c) mixture of MWCNTs (0.05 mg mL^{-1}) and CNB-90 (0.1 mg mL^{-1}), d) mixture of MWCNTs (0.2 mg mL^{-1}) and CNB-90 (0.1 mg mL^{-1}), e) cryo-TEM image of the sample in (c). Expansions indicate the binding of CNBs to CNTs.

not agglomerated MWCNTs, but a superstructural network of MWCNTs/CNBs. The cryo-TEM measurement of this stable dispersion in Figure 2e visualizes the disentangled CNTs, which are surrounded by CNBs; thus, the attachment of CNBs to CNTs is not a drying artifact, but prevails in the real solution state. Moreover, free CNBs were observed as well, which is in agreement with the aforementioned TEM characterization.

At the same CNB content, but increasing the CNT concentration from 0.05 to 0.2 mg mL^{-1} (Figure 2d), the carbon materials formed a new structure that was so extended as to settle down at the bottom, leaving a slightly grey transparent solution containing only traces of CNBs. Similar behavior is well known from coacervates and polyelectrolyte complexes: soluble structures are only obtained when one of the components is in excess; for structurally balanced compositions, extended aggregates precipitate.[7] In such a structure, the MWCNTs act as the network backbone and individual CNBs as crosslinkers to lock the 3D framework of the resulting overall structure (see TEM image in Figure S2).

At a lower CNT concentration (Figure 2c), and thus a higher CNB/CNT ratio, CNTs are quite diluted, which makes them statistically bind to a number of CNBs, but most CNBs only bind to one CNT. As mentioned before, even at this level of dilution, a small fraction of precipitate was observed. TEM characterization of this precipitate (Figure S3) again revealed a CNT/CNB network. All of these observations point to a specific interaction between CNTs and CNBs that is very similar to polyelectrolyte complex formation.

To clarify this unusual carbon–carbon interaction in aqueous solution, zeta potential measurements were performed. The CNB surface is negatively charged (−36 mV), and so they are fairly stable in pH-neutral aqueous solution. The zeta potential measured for the stable CNB/CNT dispersion (Figure 2c) is −41 mV, which is even higher than the pure CNB one; this suggests that a cooperative stabilization occurs. We attribute this to a donor/acceptor-like interaction of the two conjugated carbon nanostructures. As the CNBs are nitrogen-doped and are therefore rather electron poor (the electrons have a lower Fermi level), charge density is transferred from the CNTs to the CNBs, and the CNTs become positively charged, while the CNBs are even more negatively charged. The spontaneous polarization also occurs in the water phase: the CNBs act as an electron poor Lewis acid and attract hydroxyl ions to increase their electron density.[8] Such charge transfer holds the two nanostructures together and creates coacervates, which are observed here by electron microscopy.

The interaction of different carbon nanostructures has recently been reported by several groups. For example, Huang et al. and Dong et al. demonstrate the stabilization of CNTs by graphene oxide (GO) in the aqueous phase;[8] Tang et al. presented the structure–stability relationship for graphene-wrapped fullerene-coated CNTs;[9] Shao et al. used GO and CNT interactions to create carbon membranes.[10] The mechanism was assigned to either the intrinsic amphiphilicity in one of the carbon nanostructures, or the π–π interaction between two different carbons.

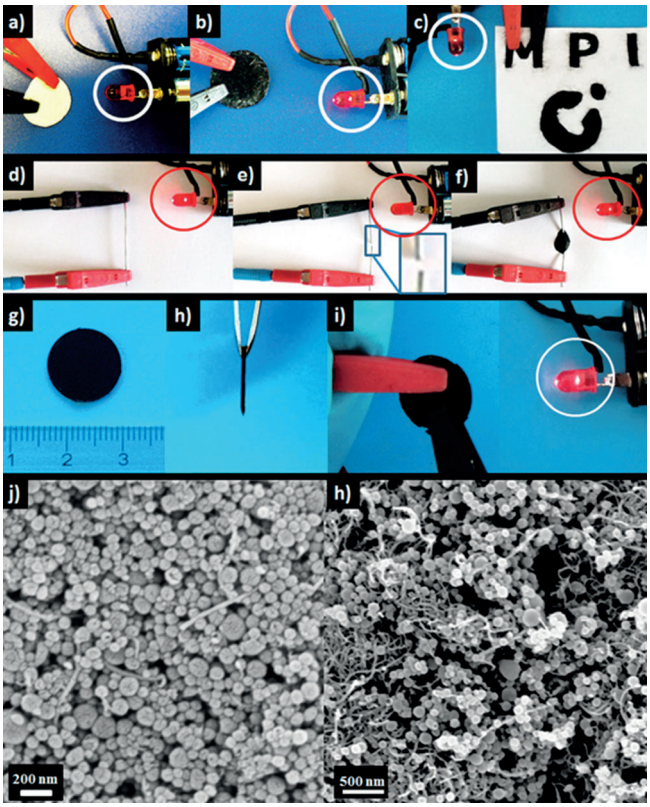

Figure 3. Photographs of a) pristine cellulose filter membrane, b) conductive membrane formed by depositing the CNT/CNB network onto the filter paper, c) filter paper with a conductive pattern, d–f) current conduction through a cut copper wire by conductive ink made from a concentrated CNT/CNB mixture, g,h) front and side views of a carbon disc, and i) a conductive carbon disc transmitting energy to an LED lamp. j,k) SEM images of the surface and cross-sectional structure of the carbon disc, reveling the complex local structure.

The distinctive CNB–CNT interaction can be applied to generate conductive carbon products of various forms, such as membranes. Normal cellulose filter membranes are electrical isolators (Figure 3a). By filtration of a mixture of MWCNTs and CNB-90 (Figure 2c) through a membrane filter, the CNT/CNB superstructures were deposited on the upper filter surface. After drying, the structure was able to act as an effective electron conductor, as illustrated by closing the circuit of an LED lamp (Figure 3b). The apparent conductivity was measured to be 10–100 S m^{-1}, depending on the estimated thickness of the conductive zone on top of the filter membrane. On the one hand, such a membrane preserves the high mechanical flexibility of the original filter membrane and can be reversibly bent without harming the conductivity. On the other hand, it is easily patternable by using a mask during filtration (Figure 3c), or by dual-color printing. It should be noted that the same membrane processing method is inapplicable to either pristine MWCNTs, owing to their poor dispersability in water, or CNBs, owing to their rather small size, which allows them to penetrate filter membranes.

Aside from filter membranes, purely carbon-based conductive inks could be produced as well. To reach the necessary high concentration, mechanical grinding of a mixture of

MWCNTs (10 mg) and CNB-90 (10 mg) in a minimum amount of water (0.5 mL) was used instead of sonication. This provides a fluid-processable ink that can be deposited to connect a cut copper wire (Figure 3d–f; see also Figure S4). Unlike MWCNTs, the CNBs themselves are well dispersible in water and can build up conductive inks in the same way. However, owing to the spherical particle morphology, a higher concentration of CNBs than that in the CNB/MWCNT mixture is needed to achieve conductance.

Finally, thin porous carbon plates were made from MWCNTs and CNB-90 by collecting and drying the superstructural network from their dispersion and pressing the dried powder (with 5 MPa) into a regular shape. MWCNTs cannot be processed in this manner, as the shaped objects collapse once the mold is released. CNBs form a regularly shaped yet rather fragile carbon product because of the lack of mechanically robust CNT network junctions. Figure 3g–h shows a centimeter-sized disc of 0.4 mm thickness. With a normal pressing setup for Fourier infrared spectroscopy, we could manage discs as thin as 0.1 mm. The solid structure of the disc was analyzed by scanning electron microscopy (SEM). As shown in Figure 3j, the film exterior presents a CNB-rich smooth plain, because CNBs favorably cover the CNT surface. In contrast, the cross-sectional view reveals a homogeneous blend of CNBs and CNTs on a submicron level, that is, the primary complex particles can rearrange in the wet state and form a homogeneous conductive network. The carbon discs built up from the CNB-90 and MWCNTs at different weight ratios (weight content of MWCNTs: 50–100%) exhibit an electron conductivity of 1000–1700 $S\,m^{-1}$ (Figure S5). A mixture of MWCNTs and cetyl trimethyl ammonium bromide (CTAB) as stabilizer (weight ratio ca. 1:1) could be shaped into discs in a similar way, but their thermal stability and corrosion resistance against organic solvents are poor because of the CTAB fraction. Nitrogen sorption isotherms were plotted to determine the accessible Brunauer–Emmett–Teller specific surface area (S_{BET}) of the membrane (Figure S6). A S_{BET} value of 420 $m^2 g^{-1}$ was obtained, which is not only higher than the CNB-90 (130 $m^2 g^{-1}$), but also than the pristine MWCNTs (280 $m^2 g^{-1}$), reflecting the more disentangled solid state of the MWCNTs. As a control experiment, a film created from a similarly treated mixture of MWCNTs and silica nanoparticles (Ludox AS-40) has a S_{BET} of only 175 $m^2 g^{-1}$ (Table S1).

In summary, we have reported the surfactant-free stabilization effect of carbon nanotubes in the presence of nitrogen-doped carbon nanobubbles in water. We attribute both colloidal stability and coacervate formation to spontaneous charge transfer from the electron-rich CNTs to the electron-poor CNBs by donor–acceptor-like π–π interactions. This phenomenon could be utilized to prepare conductive membranes from filter papers, as well as all-carbon-based inks, solders, and films. The π–π interaction between these two different carbon nanostructures might be of special interest for future work, as it not only binds these two nanostructures together in aqueous phase, but also creates a new type of carbon p–n junction that can be used to improve charge separation. Furthermore, this stabilization can be readily extended from carbon nanotubes to other aromatic carbon systems, such as graphene and fullerenes.

Received: August 24, 2013
Revised: October 1, 2013
Published online: December 5, 2013

Keywords: conducting materials · membranes · nanostructures · nitrogen-doped carbon · stabilization

[1] Q. Cao, J. A. Rogers, *Adv. Mater.* **2009**, *21*, 29–53.
[2] A. Bianco, K. Kostarelos, M. Prato, *Curr. Opin. Chem. Biol.* **2005**, *9*, 674–679.
[3] J. N. Coleman, U. Khan, Y. K. Gun'ko, *Adv. Mater.* **2006**, *18*, 689–706.
[4] P. W. Barone, S. Baik, D. A. Heller, M. S. Strano, *Nat. Mater.* **2005**, *4*, 86–92.
[5] a) C. Galeano, J. C. Meier, V. Peinecke, H. Bongard, I. Katsounaros, A. A. Topalov, A. Lu, K. J. J. Mayrhofer, F. Schüth, *J. Am. Chem. Soc.* **2012**, *134*, 20457–20465; b) G.-P. Hao, W.-C. Li, D. Qian, G.-H. Wang, W.-P. Zhang, T. Zhang, A.-Q. Wang, F. Schüth, H.-J. Bongard, A.-H. Lu, *J. Am. Chem. Soc.* **2011**, *133*, 11378–11388; c) A.-H. Lu, J.-J. Nitz, M. Comotti, C. Weidenthaler, K. Schlichte, C. W. Lehmann, O. Terasaki, F. Schüth, *J. Am. Chem. Soc.* **2010**, *132*, 14152–14162; d) R. Liu, S. M. Mahurin, C. Li, R. R. Unocic, J. C. Idrobo, H. Gao, S. J. Pennycook, S. Dai, *Angew. Chem.* **2011**, *123*, 6931–6934; *Angew. Chem. Int. Ed.* **2011**, *50*, 6799–6802; e) X. Wang, S. Dai, *Angew. Chem.* **2010**, *122*, 6814–6818; *Angew. Chem. Int. Ed.* **2010**, *49*, 6664–6668; f) Y. Zhai, Y. Dou, D. Zhao, P. F. Fulvio, R. T. Mayes, S. Dai, *Adv. Mater.* **2011**, *23*, 4828–4850; g) S. Zhang, L. Chen, S. Zhou, D. Zhao, L. Wu, *Chem. Mater.* **2010**, *22*, 3433–3440; h) Y. Fang, Y. Lv, R. Che, H. Wu, X. Zhang, D. Gu, G. Zheng, D. Zhao, *J. Am. Chem. Soc.* **2013**, *135*, 1524–1530; i) J. P. Paraknowitsch, A. Thomas, *Energy Environ. Sci.* **2013**, *6*, 2839–2855; j) J. P. Paraknowitsch, J. Zhang, D. Su, A. Thomas, M. Antonietti, *Adv. Mater.* **2010**, *22*, 87–92; k) T.-P. Fellinger, A. Thomas, J. Yuan, M. Antonietti, *Adv. Mater.* **2013**, *25*, 5838–5855; l) X. Feng, Y. Liang, L. Zhi, A. Thomas, D. Wu, I. Lieberwirth, U. Kolb, K. Müllen, *Adv. Funct. Mater.* **2009**, *19*, 2125–2129; m) R. Li, K. Parvez, F. Hinkel, X. Feng, K. Müllen, *Angew. Chem.* **2013**, *125*, 5645–5648; *Angew. Chem. Int. Ed.* **2013**, *52*, 5535–5538; n) Z.-S. Wu, Y. Sun, Y.-Z. Tan, S. Yang, X. Feng, K. Müllen, *J. Am. Chem. Soc.* **2012**, *134*, 19532–19535; o) M. Antonietti, K. Müllen, *Adv. Mater.* **2010**, *22*, 787–787; p) H.-W. Liang, Q.-F. Guan, L.-F. Chen, Z. Zhu, W.-J. Zhang, S.-H. Yu, *Angew. Chem.* **2012**, *124*, 5191–5195; *Angew. Chem. Int. Ed.* **2012**, *51*, 5101–5105; q) P. Chen, T.-Y. Xiao, H.-H. Li, J.-J. Yang, Z. Wang, H.-B. Yao, S.-H. Yu, *ACS Nano* **2012**, *6*, 712–719; r) L.-F. Chen, X.-D. Zhang, H.-W. Liang, M. Kong, Q.-F. Guan, P. Chen, Z.-Y. Wu, S.-H. Yu, *ACS Nano* **2012**, *6*, 7092–7102; s) D. Carriazo, M. C. Gutiérrez, R. Jiménez, M. L. Ferrer, F. Del Monte, *Part. Part. Syst. Charact.* **2013**, *30*, 316–320; t) D. Carriazo, M. C. Gutiérrez, F. Picó, J. M. Rojo, J. L. G. Fierro, M. L. Ferrer, F. del Monte, *ChemSusChem* **2012**, *5*, 1405–1409; u) D. Carriazo, F. Pico, M. C. Gutierrez, F. Rubio, J. M. Rojo, F. del Monte, *J. Mater. Chem.* **2010**, *20*, 773–780; v) K. K. R. Datta, V. V. Balasubramanian, K. Ariga, T. Mori, A. Vinu, *Chem. Eur. J.* **2011**, *17*, 3390–3397; w) D. S. Dhawale, M. R. Benzigar, M. A. Wahab, C. Anand, S. Varghese, V. V. Balasubramanian, S. S. Aldeyab, K. Ariga, A. Vinu, *Electrochim. Acta* **2012**, *77*, 256–261; x) D. S. Dhawale, G. P. Mane, S. Joseph, C. Anand, K. Ariga, A. Vinu, *ChemPhysChem* **2013**, *14*, 1563–1569; y) M. A. Hunt, T. Saito, R. H. Brown, A. S. Kumbhar, A. K. Naskar, *Adv. Mater.* **2012**, *24*, 2386–2389; z) R. R. Kohlmeyer, M. Lor, J. Deng, H.

Liu, J. Chen, *Carbon* **2011**, *49*, 2352 – 2361; aa) D. H. Lee, J. E. Kim, T. H. Han, J. W. Hwang, S. Jeon, S.-Y. Choi, S. H. Hong, W. J. Lee, R. S. Ruoff, S. O. Kim, *Adv. Mater.* **2010**, *22*, 1247 – 1252; ab) Q. Liu, H. Zhang, H. Zhong, S. Zhang, S. Chen, *Electrochim. Acta* **2012**, *81*, 313 – 320; ac) B. F. Machado, P. Serp, *Catal. Sci. Technol.* **2012**, *2*, 54 – 75; ad) H. D. Pham, V. H. Pham, T. V. Cuong, T.-D. Nguyen-Phan, J. S. Chung, E. W. Shin, S. Kim, *Chem. Commun.* **2011**, *47*, 9672 – 9674; ae) D. Saha, E. A. Payzant, A. S. Kumbhar, A. K. Naskar, *ACS Appl. Mater. Interfaces* **2013**, *5*, 5868 – 5874; af) F. Su, C. K. Poh, J. S. Chen, G. Xu, D. Wang, Q. Li, J. Lin, X. W. Lou, *Energy Environ. Sci.* **2011**, *4*, 717 – 724; ag) S. K. Vashist, D. Zheng, K. Al-Rubeaan, J. H. T. Luong, F.-S. Sheu, *Biotechnol. Adv.* **2011**, *29*, 169 – 188; ah) X. Xie, M. Ye, L. Hu, N. Liu, J. R. McDonough, W. Chen, H. N. Alshareef, C. S. Criddle, Y. Cui, *Energy Environ. Sci.* **2012**, *5*, 5265 – 5270; ai) B. You, L. Wang, L. Yao, J. Yang, *Chem. Commun.* **2013**, *49*, 5016 – 5018; aj) R. Zhang, Q. Wen, W. Qian, D. S. Su, Q. Zhang, F. Wei, *Adv. Mater.* **2011**, *23*, 3387 – 3391; ak) Y. Zhong, M. Jaidann, Y. Zhang, G. Zhang, H. Liu, M. Ioan Ionescu, R. Li, X. Sun, H. Abou-Rachid, L.-S. Lussier, *J. Phys. Chem. Solids* **2010**, *71*, 134 – 139; al) D.-D. Zhou, Y.-J. Du, Y.-F. Song, Y.-G. Wang, C.-X. Wang, Y.-Y. Xia, *J. Mater. Chem. A* **2013**, *1*, 1192 – 1200.

[6] S. Soll, T.-P. Fellinger, X. Wang, Q. Zhao, M. Antonietti, J. Yuan, *Small* **2013**, DOI: 10.1002/smll.201300680.

[7] E. Kizilay, A. B. Kayitmazer, P. L. Dubin, *Adv. Colloid Interface Sci.* **2011**, *167*, 24 – 37.

[8] a) X. H. Li, M. Antonietti, *Chem. Soc. Rev.* **2012**, *41*, 65936604; b) M. S. Fuhrer, J. Nygdrd, L. Shih, M. Bockrath, A. Zettl, P. McEuen, *Physica E* **2000**, *6*, 868 – 871; c) Z. Yao, H. Postma, L. Balents, C. Dekker, *Nature* **1999**, *402*, 273 – 276; d) A. A. Odintsov, "Charge transfer phenomena in carbon nanotube heterodevices", 8th Int. Symp. "Nanostructures: Physics and Technology", St Petersburg, Russia, June 19 – 23, **2000**, pp. 478 – 482; e) Q. Wang, S.-W. Yang, Y. Yang, M. B. Chan-Park, Y. Chen, *J. Phys. Chem. Lett.* **2011**, *2*, 1009 – 1014; f) G. L. C. Paulus, Q. H. Wang, Z. W. Ulissi, T. P. McNicholas, A. Vijayaraghavan, C.-J. Shih, Z. Jin, M. S. Strano, *Small* **2013**, *9*, 1954 – 1963.

[9] a) L. J. Cote, J. Kim, V. C. Tung, J. Luo, F. Kim, J. Huang, *Pure Appl. Chem.* **2011**, *83*, 95 – 110; b) X. Dong, G. Xing, M. B. Chan-Park, W. Shi, N. Xiao, J. Wang, Q. Yan, T. C. Sum, W. Huang, P. Chen, *Carbon* **2011**, *49*, 5071 – 5078; c) V. C. Tung, J. H. Huang, J. Kim, A. J. Smith, C. W. Chu, J. Huang, *Energy Environ. Sci.* **2012**, *5*, 7810 – 7818; d) V. C. Tung, J.-H. Huang, I. Tevis, F. Kim, J. Kim, C.-W. Chu, S. I. Stupp, J. Huang, *J. Am. Chem. Soc.* **2011**, *133*, 4940 – 4947.

[10] C. Tang, T. Oppenheim, V. C. Tung, A. Martini, *Carbon* **2013**, *61*, 458 – 466.

[11] J.-J. Shao, W. Lv, Q. Guo, C. Zhang, Q. Xu, Q.-H. Yang, F. Kang, *Chem. Commun.* **2012**, *48*, 3706 – 3708.